

# A Putative Single-Photon Emission CT Imaging Tracer for Erythropoietin-Producing Hepatocellular A2 Receptor

Takenori Furukawa, Hiroyuki Kimura,\* Hanae Torimoto, Yusuke Yagi, Hidekazu Kawashima, Kenji Arimitsu, and Hiroyuki Yasui

Cite This: <https://doi.org/10.1021/acsmedchemlett.1c00030>

Read Online

ACCESS |

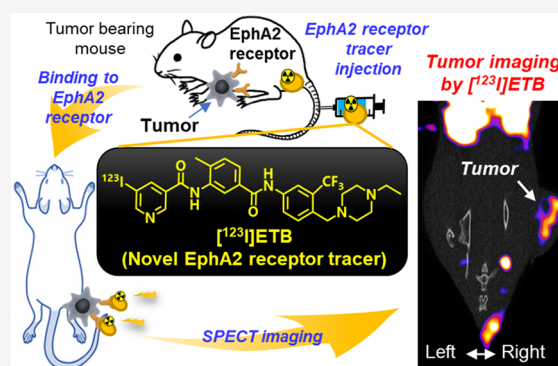
Metrics & More

Article Recommendations

Supporting Information

**ABSTRACT:** Erythropoietin-producing hepatocellular (Eph) receptors are receptor tyrosine kinases involved in cell–cell contact. The EphA2 receptor is associated with cancer proliferation and migration. Therefore, EphA2 receptor imaging has the potential for cancer diagnosis. Here, we synthesized *N*-(5-((4-(4-ethylpiperazin-1-yl)methyl)-3-(trifluoromethyl)phenyl)carbamoyl)-2-methylphenyl)-5-[<sup>123</sup>I]iodonicotinamide ([<sup>123</sup>I]ETB) and evaluated it as an imaging tracer for single-photon emission computed tomography (SPECT) imaging of the EphA2 receptor. [<sup>123</sup>I]ETB was designed on the basis of ALW-II-41-27, an inhibitor of EphA2 receptor kinase. Nonradioactive ETB was also synthesized and has been shown to efficiently inhibit EphA2 receptor kinase activity *in vitro* (IC<sub>50</sub>: ETB, 90.2 ± 18.9 nM). A cell-binding assay demonstrated that [<sup>125</sup>I]ETB binds specifically to the EphA2 receptor. The *ex vivo* biodistribution study of [<sup>125</sup>I]ETB in U87MG tumor-bearing mice also revealed tumor uptake (2.2% ID/g at 240 min). In addition, [<sup>123</sup>I]ETB uptake in tumors was visualized via SPECT/CT imaging. On the basis of the above, [<sup>123</sup>I]ETB can be considered a potential SPECT imaging tracer for the EphA2 receptor.

**KEYWORDS:** EphA2 receptor, SPECT imaging tracer, ALW-II-41-27, I-123, docking simulation



Erythropoietin-producing hepatocellular (Eph) receptor, a family of receptor tyrosine kinases,<sup>1</sup> is divided into nine EphA and five EphB subgroups defined in the human genome.<sup>2,3</sup> Eph receptors and their ephrin ligands are bound to cell membranes, and their binding causes dimerization and subsequent activation.<sup>4–7</sup> On the basis of these mechanisms, it was hypothesized that the Eph receptor is related to migration and permeation of cancer cells. This study focused on the EphA2 receptor as it was determined to be particularly overexpressed in cancer cells than in normal cells. Furthermore, the EphA2 receptor has been reportedly expressed in various types of cancer, including breast and prostate cancer and malignant gliomas.<sup>8–10</sup> Additionally, cell migration was increased by introducing a vector of EphA2 receptor into a cancer cell line that does not express the EphA2 receptor.<sup>11</sup> Although our understanding of the EphA2 receptor has advanced, its detailed mechanisms are yet to be fully understood.<sup>7,11,12</sup> Therefore, a method for performing non-invasive measurement of the distribution and density of the EphA2 receptor in tumors could provide useful information for diagnosing cancer, which in turn can contribute to the development of therapeutic drugs. From the viewpoint of sensitivity and quantitativity, positron emission tomography (PET) and single-photon emission computed tomography (SPECT) are widely used as noninvasive imaging techniques.

The first EphA2-targeted PET imaging tracer based on peptide has recently been reported by Mudd et al.,<sup>13</sup> and its potential usefulness as an imaging tracer has been discussed. Antibodies against EphA2 receptor that are labeled with Cu-64 and Zr-89 have been also proposed for PET.<sup>14</sup> We decided to develop a SPECT imaging tracer because of its high clinical versatility. Given the high number of SPECT instruments installed in medical facilities, development of SPECT imaging tracers is of great significance for clinical versatility. In addition, since a small molecule imaging tracer for EphA2 receptor has not yet been reported, we decided to develop an imaging tracer based on a small molecule. Herein, we report on an analogue of a well-established EphA2 receptor inhibitor that can be successfully labeled with I-123 and serve as a potential EphA2 receptor-specific SPECT imaging tracer. Several compounds have been reported as EphA2 receptor inhibitors (Figure 1).<sup>15–17</sup> Among these, we decided to use ALW-II-41-27 as a scaffold, as it was reported to bind to EphA2 receptor

Received: January 17, 2021

Accepted: July 9, 2021

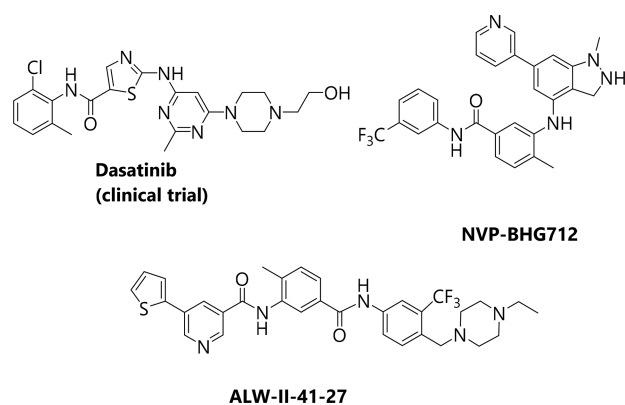


**Figure 1.** Chemical structures of previously reported EphA2 receptor inhibitors.

kinase with high affinity ( $IC_{50} = 11$  nM) and also efficiently inhibit cancer progression.<sup>15,18,19</sup> We also decided on radio-

iodination as the radiolabeling method of choice, in order to achieve minor conformational changes to our highly potent scaffold. In this context, gamma-emitting I-123 was selected for the development of our SPECT imaging tracer candidate because of its superior qualities for SPECT imaging.

We used a computational scientific approach by means of Molecular Operating Environment (Chemical Computing Group, Montreal, Canada)<sup>20</sup> to choose the best-suited iodine position in candidate compounds based on ALW-II-41-27. Because its large size, iodine needs adequate space available in order to ensure binding of the final imaging tracer to EphA2 receptor. The computer simulation predicted that ALW-II-41-27 (Figure 2A) can bind to the ATP pocket of the EphA2 receptor with  $-8.74$  kcal/mol stability (Figure 2C) and form hydrogen bonds with multiple amino acids at the vicinity (Figure 2E). We decided to substitute the thiophene group with iodine because of their comparable sizes (Figure S2) and dispensability for EphA2 receptor inhibition,<sup>15</sup> which led to the compound *N*-(5-((4-((4-ethylpiperazin-1-yl)methyl)-3-

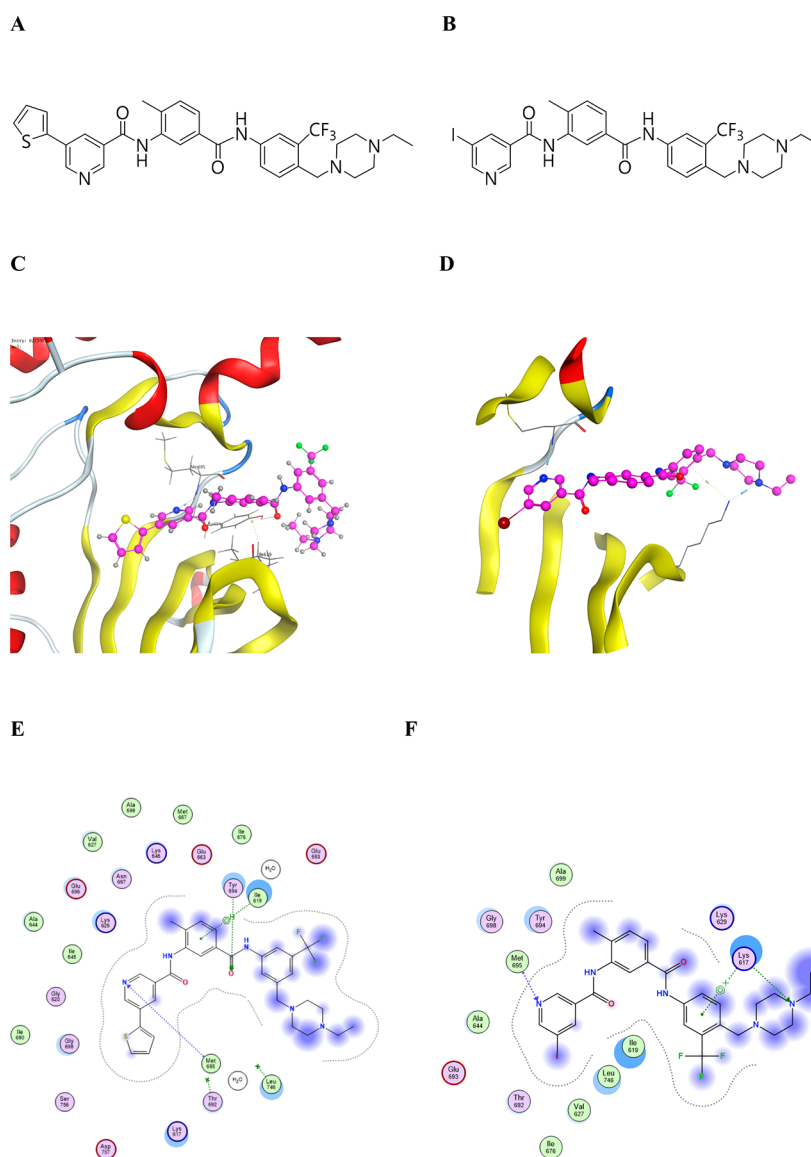
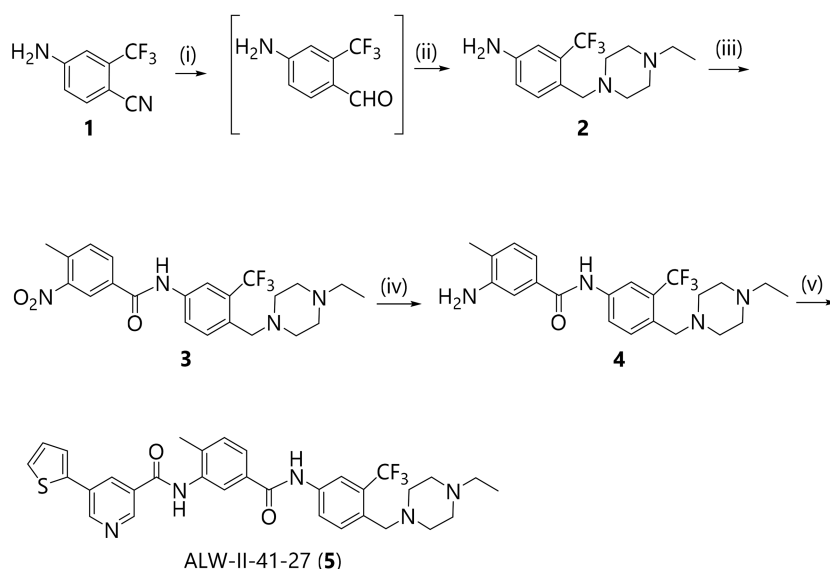
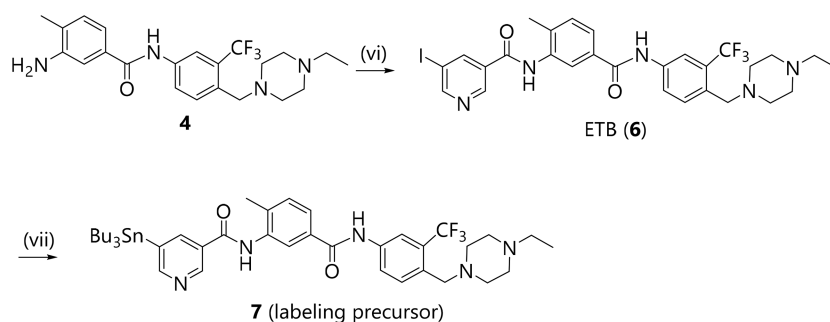


**Figure 2.** Chemical structures of inhibitors and 3D and 2D binding poses. (A, B) Chemical structures of ALW-II-41-27 and ETB. (C, D) Proposed binding mode of ALW-II-41-27 and ETB in complex with EphA2 receptor and (E, F) interaction of ALW-II-41-27 and ETB with amino acids.

A



B



(i) DIBAL-H, THF; (ii) 1-ethylpiperazine, PPTS, toluene/AcOEt reflux, then NaBH(OAc)<sub>3</sub>; (iii) 4-methyl-3-nitro benzoic acid, HATU, DMAP, DIPEA, CH<sub>2</sub>Cl<sub>2</sub>; (iv) H<sub>2</sub>, Pd/C CH<sub>2</sub>Cl<sub>2</sub>; (v) 5-thiophen-2-yl nicotinic acid, HATU, DMAP, DIPEA, CH<sub>2</sub>Cl<sub>2</sub>; (vi) 5-iodo nicotinic acid, HATU, DMAP, DIPEA, CH<sub>2</sub>Cl<sub>2</sub>; (vii) (PPh<sub>3</sub>)<sub>2</sub>Cl<sub>2</sub>Pd, Bis(tributyltin), 1,4-dioxane.

**Figure 3.** Synthetic schemes. (A) ALW-II-41-27 and (B) nonradioactive ETB and labeling precursor.

(trifluoromethyl)phenyl)carbamoyl)-2-methylphenyl)-5-iodo-nicotinamide (ETB) (Figure 2B). Computed simulation showed that ETB had a similar stability value (−8.14 kcal/mol) to that of ALW-II-41-27 for the EphA2 receptor (Figures 2D, 2F).

ALW-II-41-27 (reference standard) was synthesized using a previously reported method, as shown in Figure 3A.<sup>21–23</sup> The reduction of 4-amino-2-(trifluoromethyl)benzonitrile (**1**) with diisobutylaluminum hydride, followed by reductive amination with 1-ethylpiperazine, led to compound **2**. Aniline **2** was then reacted with 4-methyl-3-nitrobenzoic acid to obtain amide **3**. The nitro group of **3** was reduced to aniline **4**; subsequently, amidation with 5-thiophen-2-yl nicotinic acid led to ALW-II-41-27.

Nonradioactive ETB and tributyltin derivative **7** (labeling precursor) were synthesized as shown in Figure 3B. Aniline **4** was reacted with 5-iodo nicotinic acid to obtain nonradioactive ETB. Tributyltin derivative **7** was then obtained from ETB using Stille cross-coupling. ALW-II-41-27, nonradioactive ETB, and compound **7** were synthesized from compound **1** in 5.3%, 12.1%, and 9.6% yields, respectively.

The ability of the synthesized compounds to inhibit EphA2 receptor kinase activity was analyzed using an ADP-Glo kinase inhibition assay. As shown in Figure 4, nonradioactive ETB was observed to inhibit EphA2 receptor kinase activity to the same extent as ALW-II-41-27 (IC<sub>50</sub>: ALW-II-41-27, 67.2 ± 18.9 nM; ETB, 90.2 ± 18.9 nM). These results validated our drug design using computational chemistry.

C

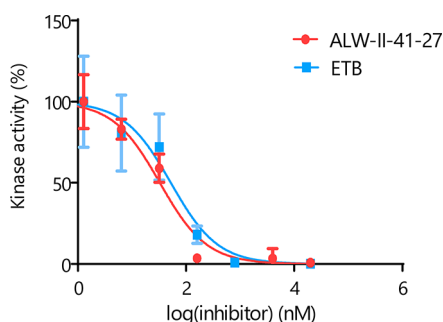


**Figure 4.** Dose-dependent inhibition of EphA2 receptor kinase using ALW-II-41-27 and ETB.

Radioiodinated [ $^{125}\text{I}$ ]ETB was obtained by iododestannylation reaction with sodium [ $^{125}\text{I}$ ]iodide and an oxidant, as per the methods described by Kimura et al. (Figure S4).<sup>24</sup> Following purification with preparative HPLC, [ $^{125}\text{I}$ ]ETB was obtained in  $70.2 \pm 1.8\%$  ( $2.9\text{--}3.1$  MBq) radiochemical yield and high radiochemical purity ( $>99\%$ ) (Figure S5B). Analytical HPLC indicated that the retention time of [ $^{125}\text{I}$ ]ETB corresponded with that of nonradioactive ETB, as shown in Figure S5B. [ $^{123}\text{I}$ ]ETB was then synthesized using sodium [ $^{123}\text{I}$ ]iodide utilizing a similar method to [ $^{125}\text{I}$ ]ETB. The radiochemical yield of [ $^{123}\text{I}$ ]ETB was determined to be  $30.1 \pm 5.6\%$  ( $25.6\text{--}59.1$  MBq), while the radiochemical purity of [ $^{123}\text{I}$ ]ETB was  $>99\%$  (Figure S23). Given the longer half-life of I-125, I-125 was used for the *ex vivo* biodistribution studies instead of I-123.

The physical properties of [ $^{125}\text{I}$ ]ETB were subsequently evaluated in order to verify suitability for use in *in vivo* testing. The octanol/water partition coefficient ( $\log D_{o/w}$ ) of [ $^{125}\text{I}$ ]ETB was determined by measuring the distribution of the radiolabeled compound in 1-octanol and phosphate-buffered saline (pH 7.4). The  $\log D_{o/w}$  of [ $^{125}\text{I}$ ]ETB was found to be 2.9 (Table S1), indicating moderate lipophilicity

and solubility in saline. The stability of [ $^{123}\text{I}$ ]ETB in mouse plasma was determined using radio-TLC analysis. [ $^{123}\text{I}$ ]ETB was determined to be stable in mouse plasma at  $37^\circ\text{C}$  for up to 4 h ( $94.5 \pm 1.5\%$ ) (Figure S24).

For the *in vitro* and *ex vivo* evaluation of [ $^{125}\text{I}$ ]ETB, the EphA2 receptor-positive U87MG cell line was used. Western blot analysis confirmed expression of the EphA2 receptor in U87MG cells and tumor xenograft tissues (Figure 6).

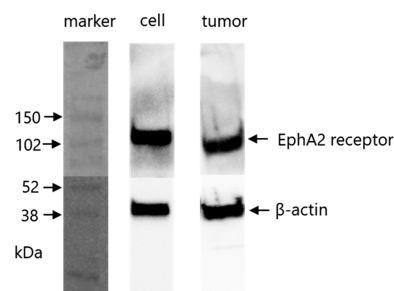


**Figure 6.** Expression of EphA2 receptor. EphA2 receptor expression in U87MG cells and tumor xenograft tissues.  $\beta$ -Actin was used as a loading control.

[ $^{125}\text{I}$ ]ETB uptake in U87MG cells is demonstrated in Figure 7. The amount of cellular uptake of [ $^{125}\text{I}$ ]ETB has been determined to increase with time ( $154.7 \pm 3.9$  cellular uptake ratio (CUR)/mg protein at 60 min,  $160.4 \pm 19.7$  CUR/mg protein at 120 min). On the contrary, the uptake of [ $^{125}\text{I}$ ]ETB significantly decreased with the addition of  $0.1\ \mu\text{M}$  of inhibitor ALW-II-41-27 (51.6% reduction at 60 min; 44.7% reduction at 120 min;  $p < 0.05$ ). This result indicated that cellular uptake of [ $^{125}\text{I}$ ]ETB is specific and EphA2-mediated. Because of its limited water solubility and toxic effect on cells,<sup>18</sup> the effective concentration of ALW-II-41-27 for receptor blockade was considered to be insufficient.

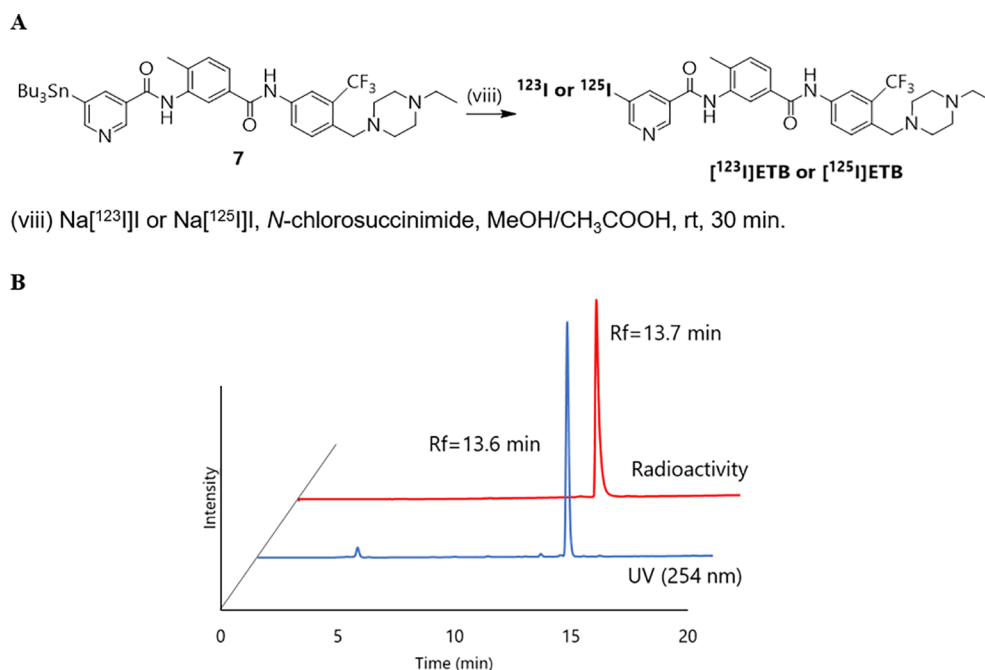


**Figure 5.** Radiosynthesis scheme and HPLC analysis. (A) Synthesis scheme of [ $^{123}\text{I}$ ]ETB or [ $^{125}\text{I}$ ]ETB and (B) HPLC analysis of nonradioactive ETB (UV) and [ $^{125}\text{I}$ ]ETB (radioactivity).

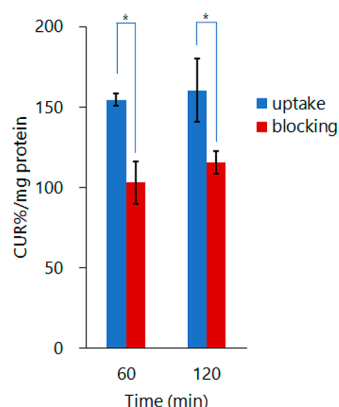


**Figure 7.** Cell-binding assay.  $[^{125}\text{I}]\text{ETB}$  CUR%/mg protein in U87MG cells. Data are represented as mean  $\pm$  SD;  $n = 5$ . \*:  $p < 0.05$  by Student's  $t$  test.

We studied the *ex vivo* biodistribution of  $[^{125}\text{I}]\text{ETB}$  in U87MG tumor-bearing mice after intravenous injection of 37 kBq/100  $\mu\text{L}$   $[^{125}\text{I}]\text{ETB}$ .  $[^{125}\text{I}]\text{ETB}$  was administered to U87MG tumor-bearing mice without anesthesia using a mouse holder. The time-course accumulation of  $[^{125}\text{I}]\text{ETB}$  in the tissues of U87MG tumor-bearing mice is presented in Figure 8 as % injected dose per gram of tissue (% ID/g). The uptake of  $[^{125}\text{I}]\text{ETB}$  by the experimental tumors was evident, reaching  $2.2 \pm 0.3\%$  ID/g at 240 min postinjection.  $[^{125}\text{I}]\text{ETB}$  was cleared rapidly from the blood, and a low level of radioactivity was observed in the heart and muscle. High renal accumulation was also observed (27.3% ID/g at 60 min postinjection), which decreased with time due to excretion (18.3% ID/g at 240 min postinjection). Furthermore, high accumulation and retention of  $[^{125}\text{I}]\text{ETB}$  in the liver was also confirmed, which can be attributed to the following reasons: (1) the compound is highly lipophilic and therefore easily taken up and retained by the liver; (2) the EphA2 receptor is highly expressed in the liver.<sup>25</sup> In addition to the liver,  $[^{125}\text{I}]\text{ETB}$  showed high accumulation and retention in the pancreas, in accordance with reports confirming EphA2 receptor expression in this tissue along with the lungs.<sup>26,27</sup> Radioactivity in the thyroid gland was found to be minimal at all time points tested ( $<0.1\%$  ID), confirming radiochemical stability *in vivo* (absence of free radioiodide) and consistent with the stability results in mouse plasma. Table 1 showed the

**Table 1.** Tumor/Blood and Tumor/Muscle Ratios of  $[^{125}\text{I}]\text{ETB}$  in U87MG Tumor-Bearing Mice after Injection

	time after injection (min)			
	30	60	120	240
tumor/blood	5.6	5.6	8.4	11.7
tumor/muscle	1.4	1.8	2.6	4.2

tumor/blood and tumor/muscle ratios for each time point (tumor/blood = 11.7 at 240 min, tumor/muscle = 4.2 at 240 min; Table 1). Compared with the previously reported  $[^{89}\text{Zr}]\text{Zr-deferoxamine-}p\text{-NCS-DS-8895a}$ ,  $[^{125}\text{I}]\text{ETB}$  was superior to  $[^{89}\text{Zr}]\text{Zr-deferoxamine-}p\text{-NCS-DS-8895a}$  in tumor/blood ratio at an early time point ( $[^{125}\text{I}]\text{ETB}$ :11.7 at 240 min,  $[^{89}\text{Zr}]\text{Zr-deferoxamine-}p\text{-NCS-DS-8895a}$ :3.62 at 7 day<sup>14</sup>).

SPECT/CT imaging was conducted in U87MG tumor-bearing mice.  $[^{123}\text{I}]\text{ETB}$  (33.62 MBq/140  $\mu\text{L}$ ) was administered intravenously to nonanesthetized U87MG tumor-bearing mice, and the mice were maintained in a nonanesthetized condition for 205 min after administration. A 5 min CT scan on an X-CUBE scanner (MOLECUBES, Ghent, Belgium) was initially performed for attenuation correction followed by a 60 min SPECT scan on  $\gamma$ -CUBE scanner (MOLECUBES, Ghent, Belgium) under anesthesia using isoflurane. As shown in Figure 9, the implanted U87MG tumors in the right limbs were clearly visualized in both dorsal and caudal images. Furthermore, in accordance with the *ex vivo* distribution data, a high accumulation of  $[^{123}\text{I}]\text{ETB}$  in the kidney was also observed.

In conclusion, we designed and synthesized an ALW-II-41-27 derivative that can be labeled with gamma-emitting I-123,  $[^{123}\text{I}]\text{ETB}$ , aiming toward the development of a potential SPECT imaging tracer targeting EphA2 receptors *in vivo*. Nonradioactive ETB is shown to inhibit EphA2 receptor kinase activity as efficiently as its parent ALW-II-41-27. The cell-binding assay performed in EphA2 receptor-positive U87MG cells, along with *in vitro* blocking with the parent ALW-II-41-27, demonstrated the specific binding of  $[^{125}\text{I}]\text{ETB}$  to the EphA2 receptor. *Ex vivo* biodistribution studies in U87MG tumor-bearing mice showed that  $[^{125}\text{I}]\text{ETB}$  is taken up by the tumor, while SPECT/CT imaging using  $[^{123}\text{I}]\text{ETB}$  in the same animal model confirmed *ex vivo* biodistribution data with a clear delineation of U87MG tumors at 205 min after injection. In view of the above,  $[^{123}\text{I}]\text{ETB}$  can be further investigated for

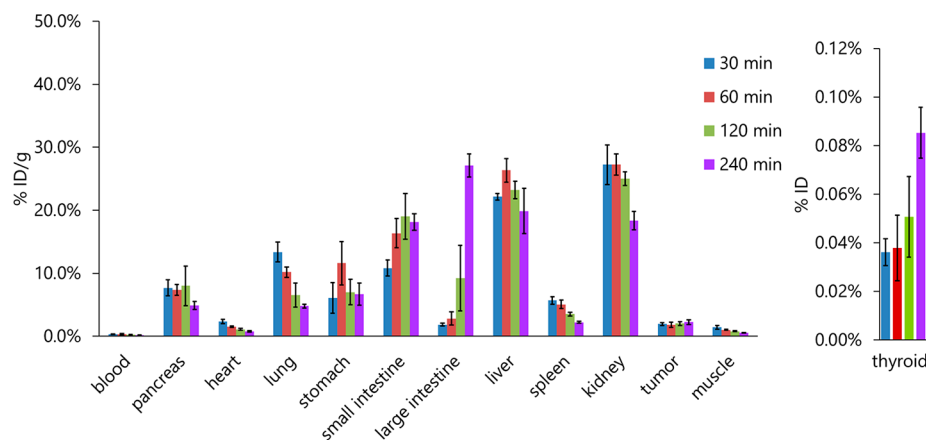


**Figure 8.** *Ex vivo* biodistribution data in U87MG tumor-bearing mice. *Ex vivo* biodistribution of  $[^{125}\text{I}]\text{ETB}$  in U87MG tumor-bearing mice at 30, 60, 120, and 240 min after injection.  $[^{125}\text{I}]\text{ETB}$  uptake in normal tissues and tumor. Data are represented as mean  $\pm$  SD;  $n = 5$ .



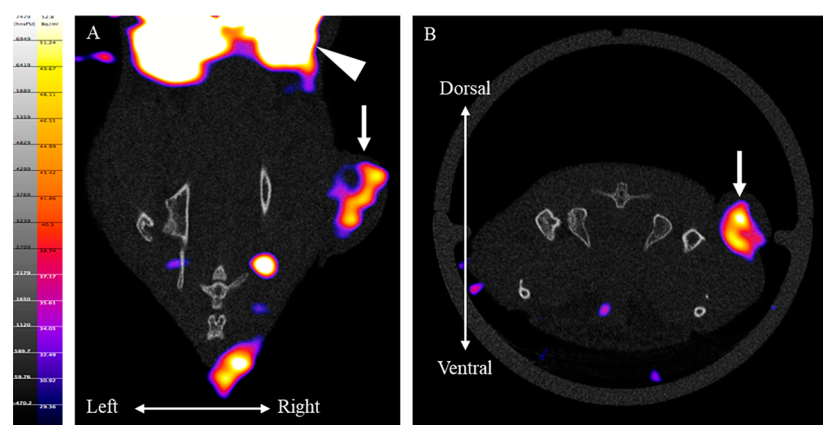


**Figure 9.** SPECT imaging of U87MG tumor-bearing mouse. Representative [ $^{123}\text{I}$ ]ETB SPECT/CT imaging in tumor-bearing mouse at 205 min after injection: (A) dorsal view and (B) caudal view image. The tumor (arrow) and the kidney (arrowhead) are shown.

its potential as a SPECT imaging tracer for EphA2 receptor-rich malignancies.

## ■ ASSOCIATED CONTENT

### Supporting Information

The Supporting Information is available free of charge at <https://pubs.acs.org/doi/10.1021/acsmchemlett.1c00030>.

Materials and methods, mass spectra, and NMR spectra (PDF)

## ■ AUTHOR INFORMATION

### Corresponding Author

**Hiroyuki Kimura** – Department of Analytical and Bioinorganic Chemistry, Division of Analytical and Physical Chemistry, Kyoto Pharmaceutical University, Kyoto 607-8414, Japan; [orcid.org/0000-0002-4291-3524](https://orcid.org/0000-0002-4291-3524); Phone: +81-75-595-4630; Email: [hkimura@mb.kyoto-phu.ac.jp](mailto:hkimura@mb.kyoto-phu.ac.jp); Fax: +81-75-595-4753

### Authors

**Takenori Furukawa** – Department of Analytical and Bioinorganic Chemistry, Division of Analytical and Physical Chemistry, Kyoto Pharmaceutical University, Kyoto 607-8414, Japan

**Hanae Torimoto** – Department of Analytical and Bioinorganic Chemistry, Division of Analytical and Physical Chemistry, Kyoto Pharmaceutical University, Kyoto 607-8414, Japan

**Yusuke Yagi** – Department of Analytical and Bioinorganic Chemistry, Division of Analytical and Physical Chemistry, Kyoto Pharmaceutical University, Kyoto 607-8414, Japan

**Hidekazu Kawashima** – Radioisotope Research Center, Kyoto Pharmaceutical University, Kyoto 607-8412, Japan

**Kenji Arimitsu** – Department of Analytical and Bioinorganic Chemistry, Division of Analytical and Physical Chemistry, Kyoto Pharmaceutical University, Kyoto 607-8414, Japan

**Hiroyuki Yasui** – Department of Analytical and Bioinorganic Chemistry, Division of Analytical and Physical Chemistry, Kyoto Pharmaceutical University, Kyoto 607-8414, Japan

Complete contact information is available at:

<https://pubs.acs.org/doi/10.1021/acsmchemlett.1c00030>

## Funding

This work was supported by Private University Research Branding Project for Ministry of Education, Culture, Sports, Science and Technology and JSPS KAKENHI Grant Number JP20K08061.

## Notes

The authors declare no competing financial interest.

## ■ ACKNOWLEDGMENTS

This work was supported by Yasunao Hattori for analysis of HRMS.

## ■ REFERENCES

- (1) Hirai, H.; Maru, Y.; Hagiwara, K.; Nishida, J.; Takaku, F. A novel putative tyrosine kinase receptor encoded by the eph gene. *Science* **1987**, *238*, 1717–1720.
- (2) Gale, N. W.; Yancopoulos, G. D. Ephrins and their receptors: a repulsive topic? *Cell Tissue Res.* **1997**, *290*, 227–241.
- (3) Miao, H.; Wang, B. Eph/ephrin signaling in epithelial development and homeostasis. *Int. J. Biochem. Cell Biol.* **2009**, *41*, 762–770.
- (4) Zhou, Y.; Sakurai, H. Emerging and diverse functions of the EphA2 noncanonical pathway in cancer progression. *Biol. Pharm. Bull.* **2017**, *40*, 1616–1624.
- (5) Pasquale, E. B. Ephrin bidirectional signaling in physiology and disease. *Cell* **2008**, *133*, 38–52.
- (6) Pasquale, E. B. Eph receptors and ephrins in cancer: bidirectional signaling and beyond. *Nat. Rev. Cancer* **2010**, *10*, 165–180.
- (7) Miao, H.; Li, D. Q.; Mukherjee, A.; Guo, H.; Petty, A.; Cutter, J.; Basilion, J. P.; Sedor, J.; Wu, J.; Danielpour, D.; Sloan, A. E.; Cohen, M. L.; Wang, B. EphA2 mediates ligand-dependent inhibition and ligand-independent promotion of cell migration and invasion via a reciprocal regulatory loop with Akt. *Cancer Cell* **2009**, *16*, 9–20.
- (8) Huang, F.; Reeves, K.; Han, X.; Fairchild, C.; Platero, S.; Wong, T. W.; Lee, F.; Shaw, P.; Clark, E. Identification of candidate molecular markers predicting sensitivity in solid tumors to dasatinib: rationale for patient selection. *Cancer Res.* **2007**, *67*, 2226–2238.
- (9) Wang, X. D.; Reeves, K.; Luo, F. R.; Xu, L. A.; Lee, F.; Clark, E.; Huang, F. Identification of candidate predictive and surrogate molecular markers for dasatinib in prostate cancer: rationale for patient selection and efficacy monitoring. *Genome Biol.* **2007**, *8*, R255.
- (10) Tandon, M.; Vemula, S. V.; Mittal, S. K. Emerging strategies for EphA2 receptor targeting for cancer therapeutics. *Expert Opin. Ther. Targets* **2011**, *15*, 31–51.
- (11) Zelinski, D. P.; Zantek, N. D.; Stewart, J. C.; Irizarry, A. R.; Kinch, M. S. EphA2 overexpression causes tumorigenesis of mammary epithelial cells. *Cancer Res.* **2001**, *61*, 2301–2306.

- (12) Macrae, M.; Neve, R. M.; Rodriguez-Viciana, P.; Haqq, C.; Yeh, J.; Chen, C.; Gray, J. W.; McCormick, F. A conditional feedback loop regulates Ras activity through EphA2. *Cancer Cell* **2005**, *8*, 111–118.
- (13) Mudd, G. E.; Brown, A.; Chen, L.; van Rietschoten, K.; Watcham, S.; Teufel, D. P.; Pavan, S.; Lani, R.; Huxley, P.; Bennett, G. S. Identification and optimization of EphA2-selective bicycles for the delivery of cytotoxic payloads. *J. Med. Chem.* **2020**, *63*, 4107–4116.
- (14) Burvenich, I. J. G.; Parakh, S.; Gan, H. K.; Lee, F. T.; Guo, N.; Rigopoulos, A.; Lee, S. T.; Gong, S.; O'Keefe, G. J.; Tochon-Danguy, H.; Kotsuma, M.; Hasegawa, J.; Senaldi, G.; Scott, A. M. Molecular Imaging and Quantitation of EphA2 Expression in Xenograft Models with <sup>89</sup>Zr-DS-8895a. *J. Nucl. Med.* **2016**, *57*, 974–980.
- (15) Miao, B.; Ji, Z.; Tan, L.; Taylor, M.; Zhang, J.; Choi, H. G.; Frederick, D. T.; Kumar, R.; Wargo, J. A.; Flaherty, K. T.; Gray, N. S.; Tsao, H. EphA2 is a Mediator of Vemurafenib Resistance and a Novel Therapeutic Target in Melanoma. *Cancer Discovery* **2015**, *5*, 274–287.
- (16) Ishigaki, H.; Minami, T.; Morimura, O.; Kitai, H.; Horio, D.; Koda, Y.; Fujimoto, E.; Negi, Y.; Nakajima, Y.; Niki, M.; Kanemura, S.; Shibata, E.; Mikami, K.; Takahashi, R.; Yokoi, T.; Kuribayashi, K.; Kijima, T. EphA2 inhibition suppresses proliferation of small-cell lung cancer cells through inducing cell cycle arrest. *Biochem. Biophys. Res. Commun.* **2019**, *519*, 846–853.
- (17) Martiny-Baron, G.; Holzer, P.; Billy, E.; Schnell, C.; Brueggen, J.; Ferretti, M.; Schmiedeberg, N.; Wood, J. M.; Furet, P.; Imbach, P. The small molecule specific EphB4 kinase inhibitor NVP-BHG712 inhibits VEGF driven angiogenesis. *Angiogenesis* **2010**, *13*, 259–267.
- (18) Martini, G.; Cardone, C.; Vitiello, P. P.; Belli, V.; Napolitano, S.; Troiani, T.; Ciardiello, D.; Della Corte, C. M.; Morgillo, F.; Matrone, N.; Sforza, V.; Papaccio, G.; Desiderio, V.; Paul, M. C.; Moreno-Viedma, V.; Normanno, N.; Rachiglio, A. M.; Tirino, V.; Maiello, E.; Latiano, T. P.; Rizzi, D.; Signoriello, G.; Sibilia, M.; Ciardiello, F.; Martinelli, E. EphA2 is a predictive biomarker of resistance and a potential therapeutic target for improving antiepidermal growth factor receptor therapy in colorectal cancer. *Mol. Cancer Ther.* **2019**, *18*, 845–855.
- (19) Amato, K. R.; Wang, S.; Hastings, A. K.; Youngblood, V. M.; Santapuram, P. R.; Chen, H.; Cates, J. M.; Colvin, D. C.; Ye, F.; Brantley-Sieders, D. M.; Cook, R. S.; Tan, L.; Gray, N. S.; Chen, J. Genetic and pharmacologic inhibition of EPHA2 promotes apoptosis in NSCLC. *J. Clin. Invest.* **2014**, *124*, 2037–2049.
- (20) *Molecular Operating Environment*, 2019.01; Chemical Computing Group ULC, 1010 Sherbrooke St. West, Suite #910, Montreal, QC, Canada, H3A 2R7, 2019.
- (21) Zhang, C. H.; Zheng, M. W.; Li, Y. P.; Lin, X. D.; Huang, M.; Zhong, L.; Li, G. B.; Zhang, R. J.; Lin, W. T.; Jiao, Y.; Wu, X. A.; Yang, J.; Xiang, R.; Chen, L. J.; Zhao, Y. L.; Cheng, W.; Wei, Y. Q.; Yang, S. Y. Design, synthesis, and structure–activity relationship studies of 3-(phenylethynyl)-1H-pyrazolo[3,4-d]pyrimidin-4-amine derivatives as a new class of Src inhibitors with potent activities in models of triple negative breast cancer. *J. Med. Chem.* **2015**, *58*, 3957–3974.
- (22) Terai, H.; Tan, L.; Beauchamp, E. M.; Hatcher, J. M.; Liu, Q.; Meyerson, M.; Gray, N. S.; Hammerman, P. S. Characterization of DDR2 inhibitors for the treatment of DDR2 mutated nonsmall cell lung cancer. *ACS Chem. Biol.* **2015**, *10*, 2687–2696.
- (23) Choi, Y.; Syeda, F.; Walker, J. R.; Finerty, P. J., Jr.; Cuerrier, D.; Wojciechowski, A.; Liu, Q.; Dhe-Paganon, S.; Gray, N. S. Discovery and structural analysis of Eph receptor tyrosine kinase inhibitors. *Bioorg. Med. Chem. Lett.* **2009**, *19*, 4467–4470.
- (24) Saji, H.; Kimura, H.; Matsumoto, H. Preparation of 2-(3-pyridinyl)-1H-benzimidazole derivatives as radiodiagnostic agents. Patent No. JP 2015193545.
- (25) Kaushansky, A.; Douglass, A. N.; Arang, N.; Vigdorovich, V.; Dambrauskas, N.; Kain, H. S.; Austin, L. S.; Sather, D. N.; Kappe, S. H. I. Malaria parasites target the hepatocyte receptor EphA2 for successful host infection. *Science* **2015**, *350*, 1089–1092.
- (26) Hong, J. Y.; Shin, M. H.; Chung, K. S.; Kim, E. Y.; Jung, J. Y.; Kang, Y. A.; Kim, Y. S.; Kim, S. K.; Chang, J.; Park, M. S. EphA2 receptor signaling mediates inflammatory responses in lipopolysaccharide-induced lung injury. *Tuberc. Respir. Dis.* **2015**, *78*, 218–226.
- (27) Blevins, K. S.; Jeong, J. H.; Ou, M.; Brumbach, J. H.; Kim, S. W. EphA2 targeting peptide tethered bioreducible poly(cystamine bisacrylamide-diamino hexane) for the delivery of therapeutic pCMV-RAE-1 $\gamma$  to pancreatic islets. *J. Controlled Release* **2012**, *158*, 115–122.